虚数化学ポテンシャルとランダム行列模型

新野康彦[A], 米山博志[B]

奈良工業高等専門学校(一般教科)[A], 佐賀大学(理工学部)[B]

九大若手研究会「量子色力学の相構造研究の現状と展望」

2008年12月25日

1. Introduction

QCD phase diagram in μ-T plane

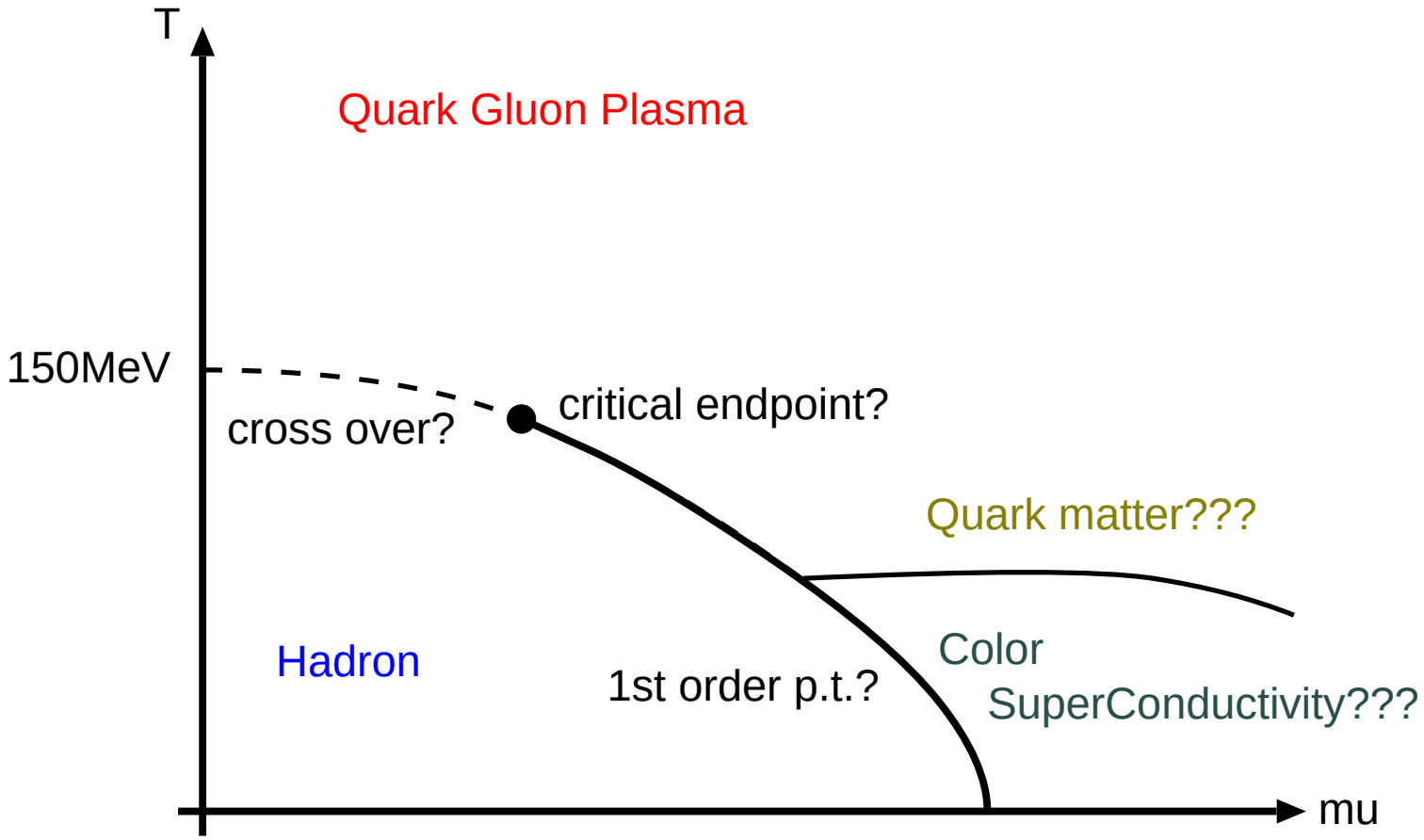

Figure 1: Skematic phase diagram in μ-Tplane.

lattice QCD

partition function: $\mathcal{Z}(\mu,T)=\int \mathcal{D}U e^{-S_G}\mathrm{det}D(U;\mu,T).$

☹ $(\mathrm{det}D(U;\mu,T))^* \neq \mathrm{det}D(U;\mu,T)$ for $\mu \neq 0.$

$\Downarrow$

sign problem

$\longrightarrow$various approaches

♣ analytic continuation from imaginary to real chemical potential

$\mu \to i\phi;\quad (\mathrm{det}D(U;i\phi,T))^* = \mathrm{det}D(U;i\phi,T). \quad \Rightarrow \quad$ *no sign problem!*

$\longrightarrow$ P. Cea et al.(2007, 2008) : study of two color QCD

and suggestion to three color QCD

P. Cea et al. (2007, 2008)

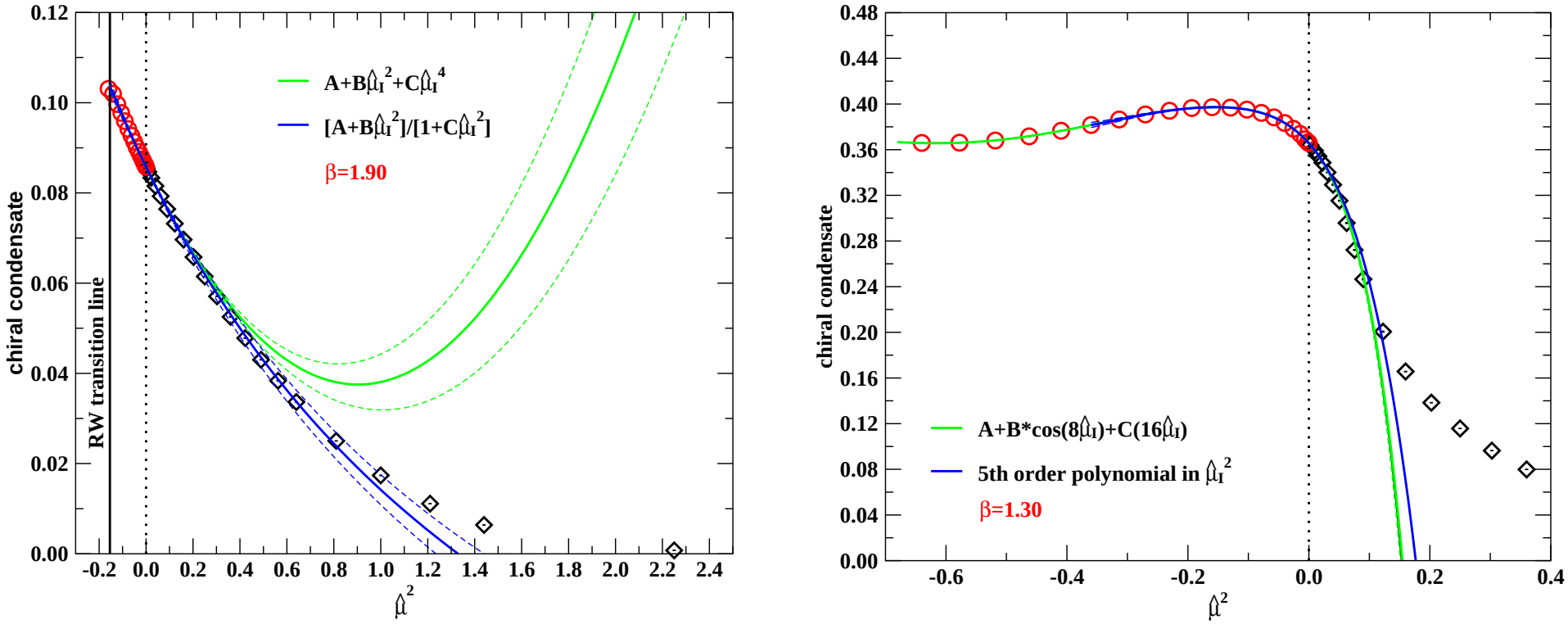

Figure 2: SU(2) gauge theory is employed with $n_f = 8$ degenerate staggered fermions and $ma = 0.07$. Figures show chiral condensate *vs.* μ^2 at $\beta = 1.90$(left) and 1.30(right). In the figures, the solid lines represent the interpolationg functions and the dashed lines give uncertainty coming from the errors in the parameters of the fit.

Our motivations

Model: two color chiral random matrix model (2-color CRMM)

- investigation of phase structure in μ_R-T and μ_I-T planes
- study of analytic continuation of chiral condensate and pseudo critical lines

2. Chiral random matrix model

chiral random matrix model (CRMM)

$$\begin{cases} -\text{describe the correlations of the low-lying eigenvalues} \\ \qquad\qquad\qquad \text{of the QCD Dirac operator} \\ -\text{an effective model for investigating QCD phase structure} \end{cases}$$

QCD partition function: $\mathcal{Z}_{QCD} = \langle \prod_{f=1}^{2} \det(D + m_f + \mu_f \gamma_0) \rangle$

- global symmetry

  2-color QCD: $\mathrm{SU}(2N_f) \to \mathrm{Sp}(2N_f) \to \mathrm{SU}_V(N_f) \times \mathrm{U}_B(1)$

- partition function

2-color CRMM: $\mathcal{Z}^{(2)}_{RMM} = \int \mathcal{D}W \exp\left[-\frac{n}{2}G^2 \mathrm{Tr} W^T W\right] \det \tilde{D}^{(2)}$

$\ddot{\smile}$ $\begin{cases} W: & \text{real } n \times n \text{ matrix} \\ \tilde{D}^{(2)} & \text{includes effects of only the lowest Matsubara frequencies.} \end{cases}$

$\Downarrow\longleftarrow$ standard manipulations

$$\mathcal{Z}^{(2)}_{RMT} = \int \mathcal{D}A e^{-\mathcal{L}} = \int \mathcal{D}A \exp\left[-\frac{n}{2}G^2 \mathrm{Tr} A^\dagger A + \frac{n}{4}\log Q^\dagger Q\right].$$

$\ddot{\smile}$ $\begin{cases} A: & \text{complex } 2N_f \times 2N_f \text{ matrix} \\ Q & \text{contains } A \text{ and effects from mass, chemical potential} \\ & \qquad\qquad\qquad \text{and temperature.} \end{cases}$

$\longrightarrow$ ansatz for A: $\quad A = \begin{pmatrix} 0 & -\sigma_1 & -i\Delta & 0 \\ \sigma_1 & 0 & 0 & -i\Delta \\ i\Delta & 0 & 0 & -\sigma_2 \\ 0 & i\Delta & \sigma_2 & 0 \end{pmatrix}$,

σ_1, σ_2: chiral condensate, Δ: diquark condensate.

$$\frac{1}{n}\mathcal{L} = 2G^2(\sigma^2+\Delta^2) - \log\left[\left\{(\sigma+m)^2+\Delta^2-\mu^2+T^2\right\}^2 + 4\mu^2(\Delta^2+T^2)\right],$$

where $m_1 = m_2 = m,\ \mu_1 = \mu_2 = \mu$ and $\sigma_1 = \sigma_2 = \sigma$ are set.

(B. Klein, D. Toublan and J. J. M. Verbaarschot (2005))

$\longrightarrow$ We investigate the phase structure in μ-T plane

by solving the saddle point equations.

3. Phase diagram in μ-T plane

saddle point equation

i) the real μ region in the $m \neq 0$ case

$$\frac{\partial \mathcal{L}}{\partial \sigma} = 0, \quad \frac{\partial \mathcal{L}}{\partial \Delta} = 0.$$

$$\begin{cases} G^2 \sigma g(m, \sigma, \Delta, \mu, T) = \left\{ (\sigma + m)^2 + \Delta^2 - \mu^2 + T^2 \right\} (\sigma + m), \\ \Delta = 0, \quad G^2 g(m, \sigma, \Delta, \mu, T) = \left\{ (\sigma + m)^2 + \Delta^2 + \mu^2 + T^2 \right\}, \end{cases}$$

$$\text{☹}\, g(m, \sigma, \Delta, \mu, T) \equiv \left\{ (\sigma + m)^2 + \Delta^2 - \mu^2 + T^2 \right\}^2 + 4\mu^2 (\Delta^2 + T^2).$$

$$\longrightarrow \begin{cases} \underline{\Omega};\ \sigma = \mathcal{O}(m),\ \Delta = 0. & \underline{\Omega^{(\Delta)}};\ \sigma = \mathcal{O}(m),\ \Delta \neq 0. \\ \underline{\Omega^{(\sigma)}};\ \sigma \neq 0,\ \Delta = 0. & \underline{\Omega^{(\Delta\sigma)}};\ \sigma \neq 0,\ \Delta \neq 0. \end{cases}$$

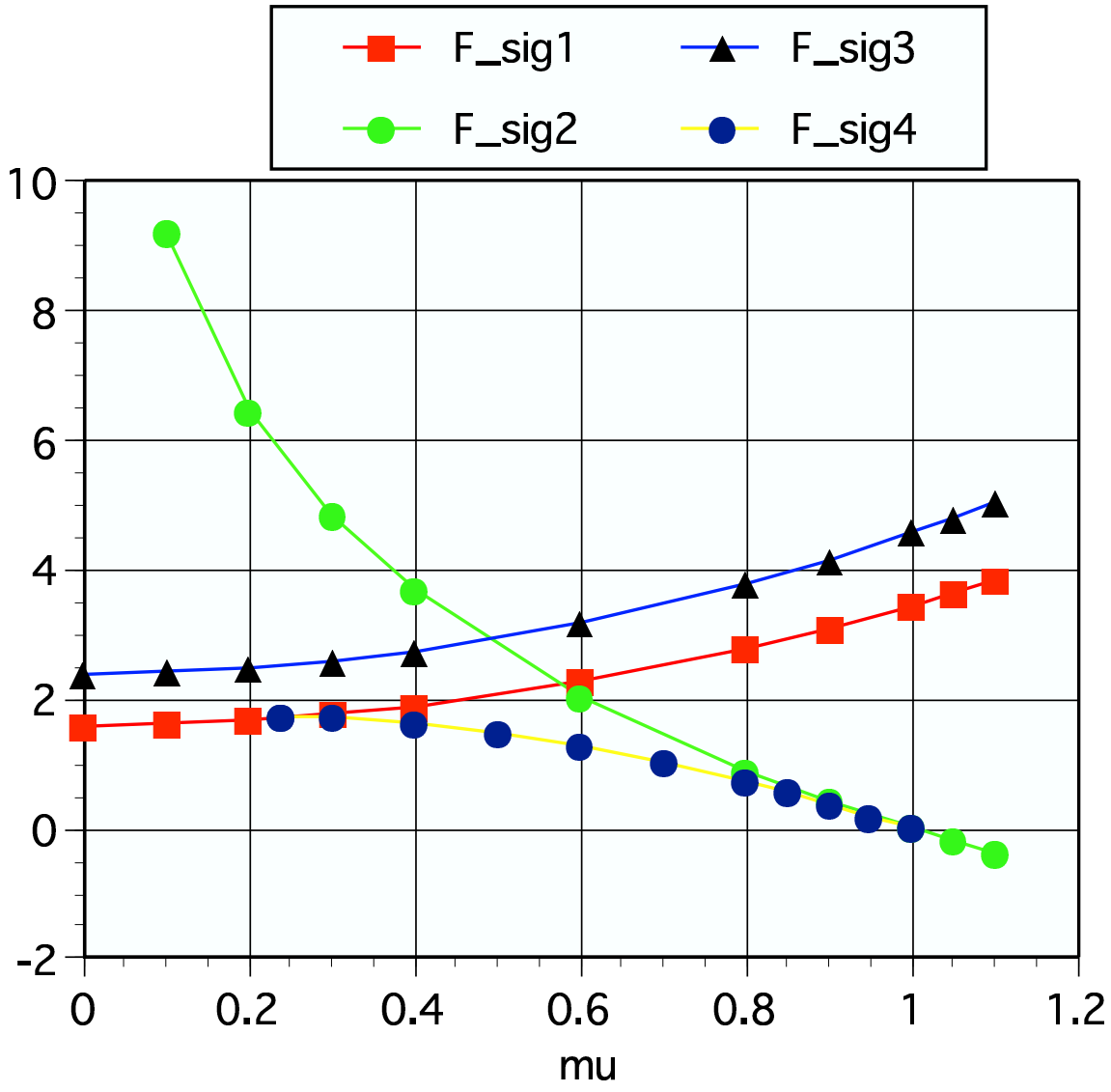

Figure 3: Effective potential for $m = 0.1$ and $T = 0$.

$$\therefore \ \Omega^{(\sigma)} \longrightarrow \Omega^{(\Delta\sigma)} \longrightarrow \Omega.$$

ii) the imaginary μ region in the $m \neq 0$ case

$$\mu \longrightarrow i\mu_I = i\phi; \quad \frac{\partial \mathcal{L}}{\partial \sigma} = 0, \quad \frac{\partial \mathcal{L}}{\partial \Delta} = 0.$$

$$\begin{cases} G^2 \sigma \tilde{g}(m, \sigma, \Delta, \phi, T) = \left\{ (\sigma + m)^2 + \Delta^2 + \phi^2 + T^2 \right\} (\sigma + m), \\ \Delta = 0, \quad G^2 \tilde{g}(m, \sigma, \Delta, \phi, T) = (\sigma + m)^2 + \Delta^2 - \phi^2 + T^2, \end{cases}$$

$$\text{☹}\, \tilde{g}(m, \sigma, \Delta, \phi, T) \equiv \left\{ (\sigma + m)^2 + \Delta^2 + \phi^2 + T^2 \right\}^2 - 4\phi^2 (\Delta^2 + T^2).$$

$$\longrightarrow \begin{cases} \underline{\tilde{\Omega}};\ \sigma = \mathcal{O}(m),\ \Delta = 0. & \underline{\tilde{\Omega}^{(\Delta)}};\ \sigma = \mathcal{O}(m),\ \Delta \neq 0. \\ \underline{\tilde{\Omega}^{(\sigma)}};\ \sigma \neq 0,\ \Delta = 0. & \underline{\tilde{\Omega}^{(\Delta\sigma)}};\ \sigma \neq 0,\ \Delta \neq 0. \end{cases}$$

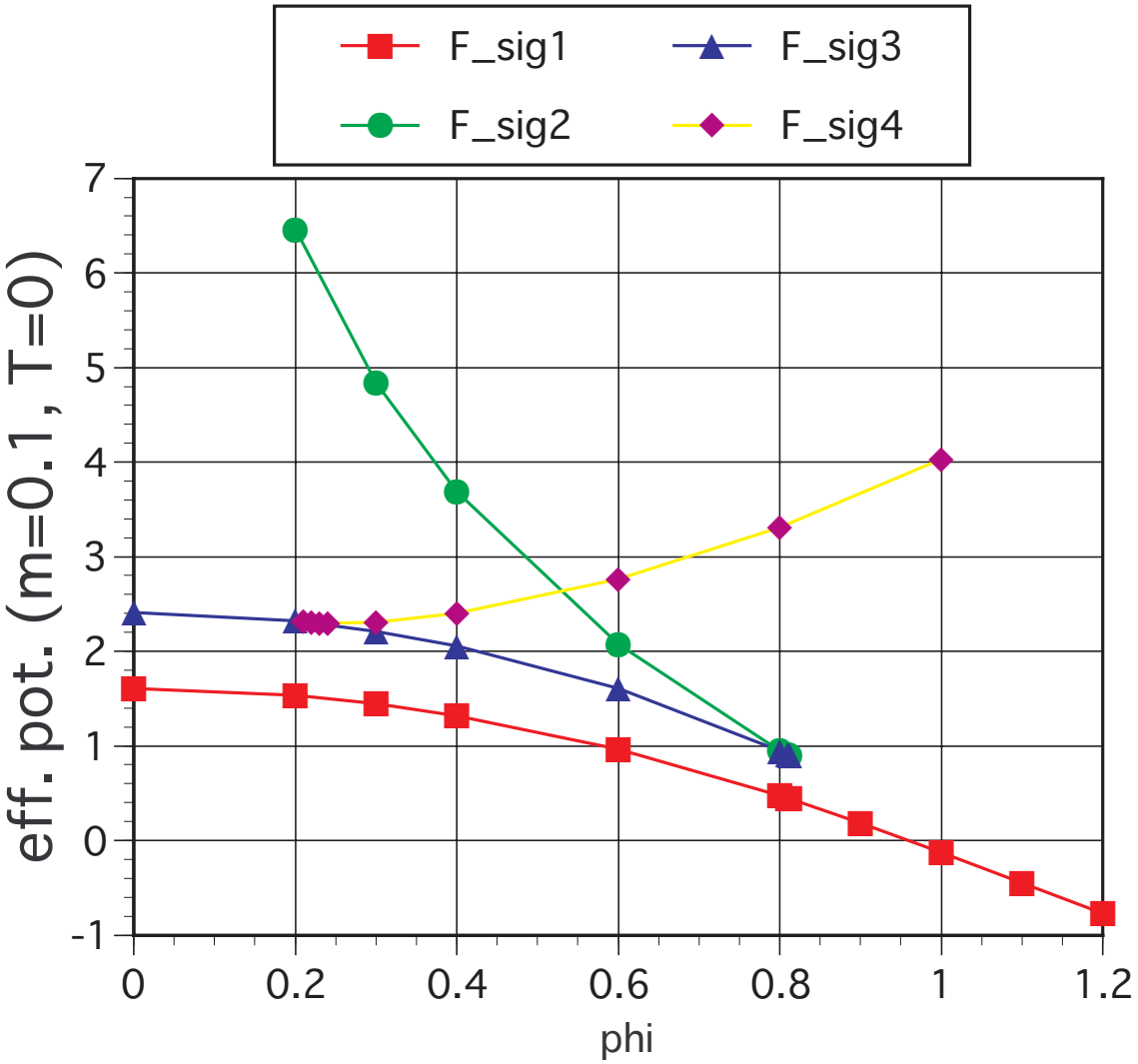

Figure 4: Effective potentials for $m = 0.1$ and $T = 0.0$.

:) chiral condensate phase is favored in μ_I region($TG \leq 1.0$).

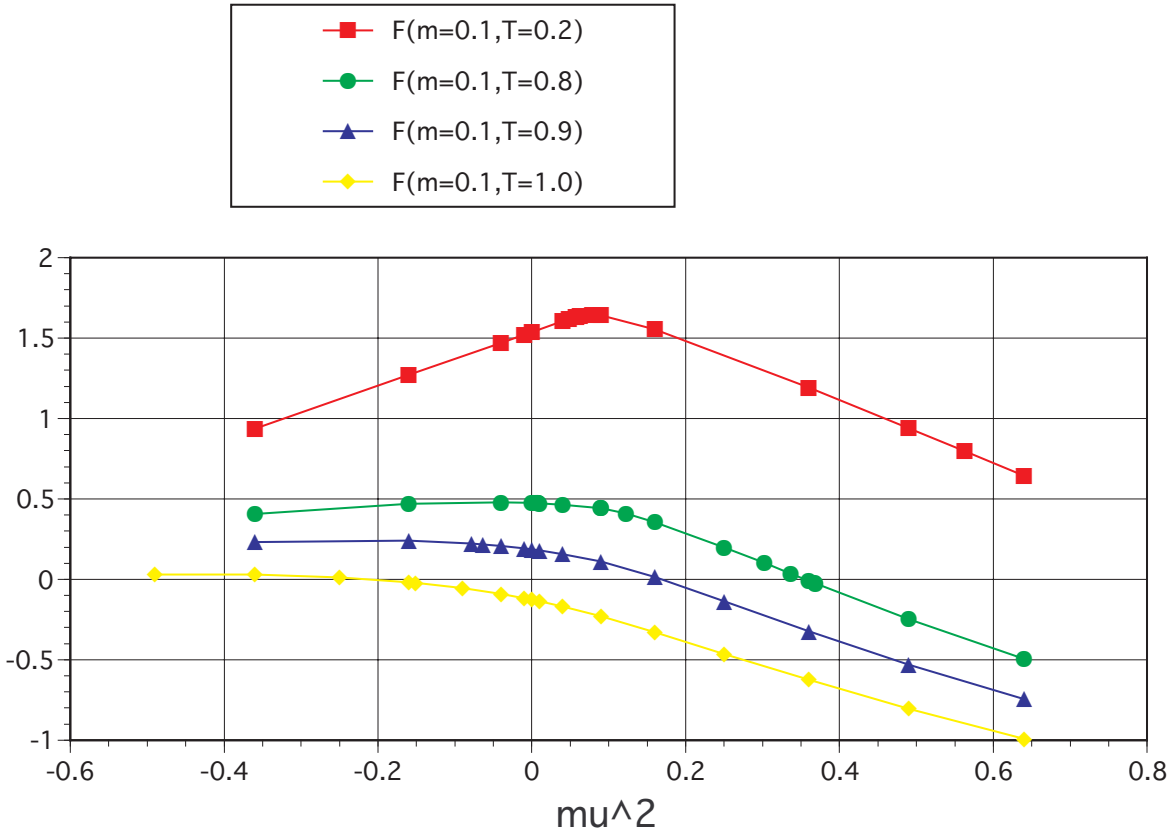

Figure 5: Free energy in real and imaginary μ regions for $m = 0.1$.

$$\text{:)}\Omega^{(\sigma)} \to \Omega^{(\Delta)} \to \Omega$$

:) free energy (the minimum value of effective potential) behaves smoothly at $\mu = 0$ for all temperatures.

phase diagram

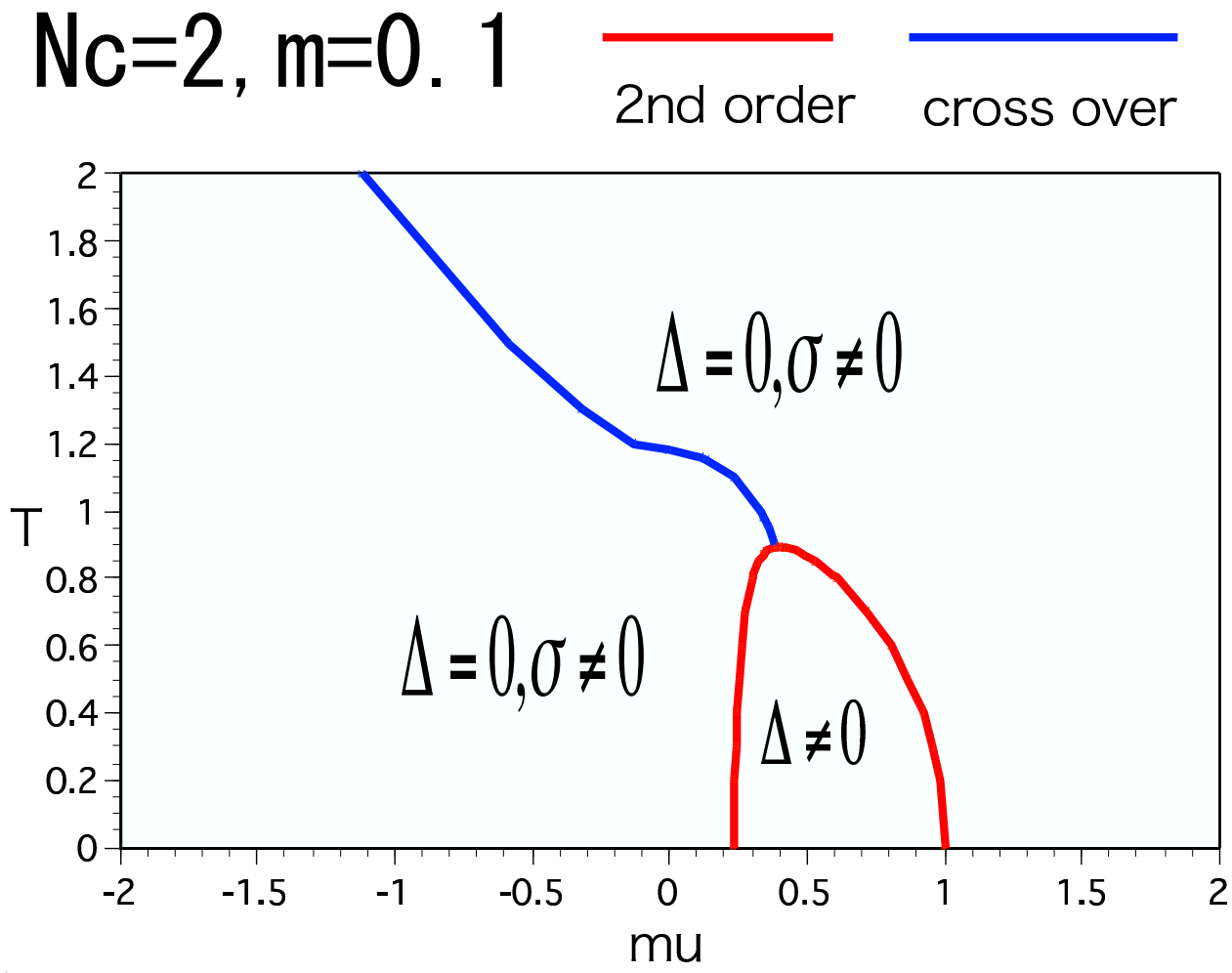

Figure 6: Phase structure for $m = 0.1$ in μ/μ_I-T plane.

4. Analytic continuation

chiral condensate

- use values of σ in a certain imaginary μ region ($\mu \to i\mu_I = i\phi$) as "data". $\Rightarrow 0 \leq \phi \leq 0.3$.

- take s points of data in a range $0 < \phi \leq \phi_f$. $\Rightarrow \ \ s = 31$ $(\Delta\phi = 0.01)$.

- fit "data" by an appropriate function and extrapolate it to the real μ region.

$$\Rightarrow \sigma(\phi) = \begin{cases} A + B\phi^2 + C\phi^4 + \cdots . & \text{(polynomial)} \\ \dfrac{A + B\phi^2}{1 + C\phi^2}. & \text{(ratio)} \end{cases}$$

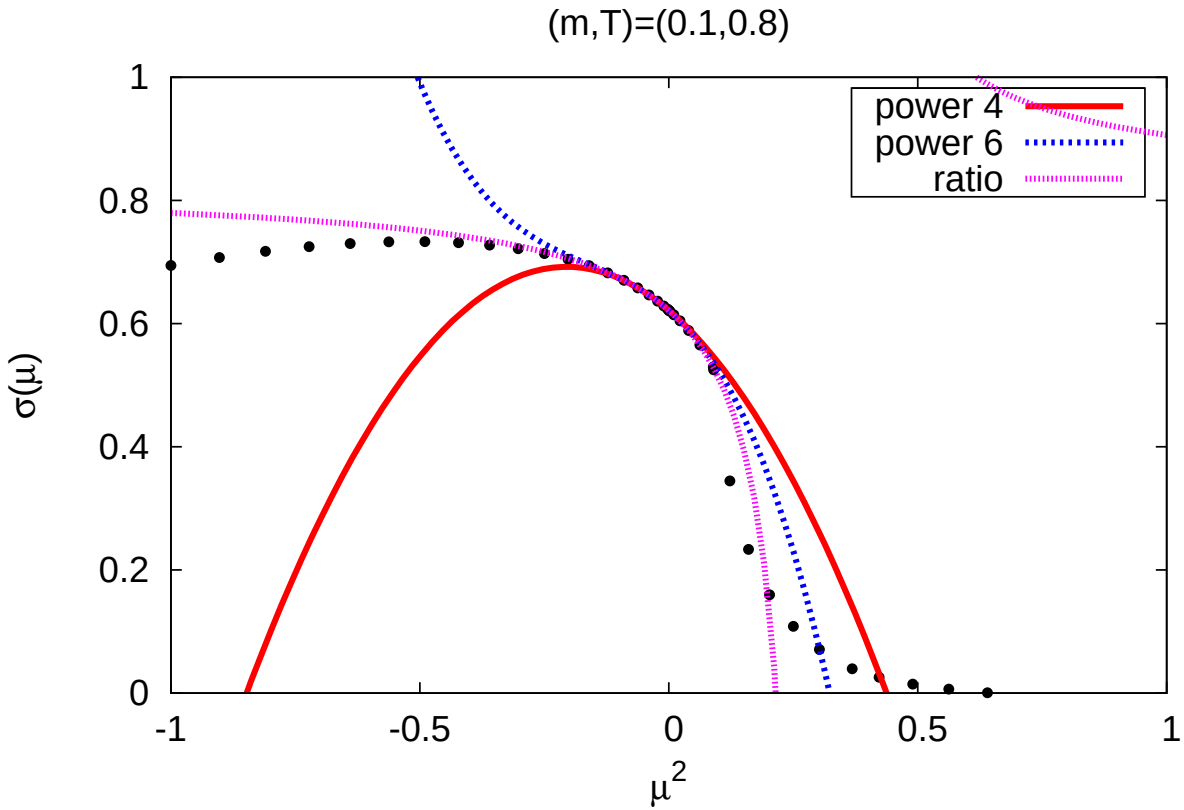

Figure 7: Chiral donsensate for $m = 0.1$ and $T = 0.8$(low temperature). For "data" in imaginary μ region, polynomials and ratio are employed as fitting functions. Note that a critical point exists at $\mu G \simeq 0.299((\mu G)^2 \simeq 0.089)$.

☺ Extrapolations for fitting functions are good up to the critical point.

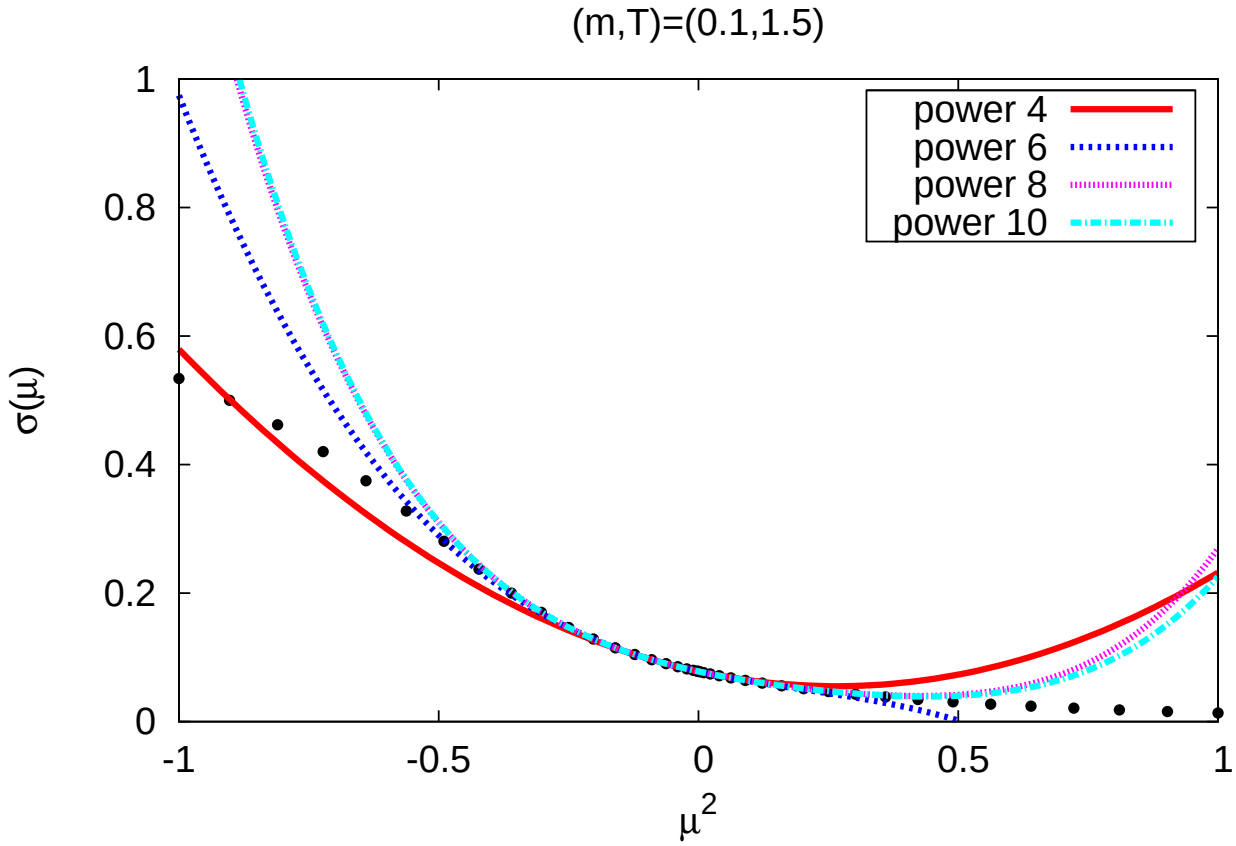

Figure 8: Chiral condensate for $m = 0.1$ and $T = 1.5$(high temperature). For "data" in imaginary μ region, polynomial fits are employed.

∴ Polynomial fit shows the behavior with slow convergence.

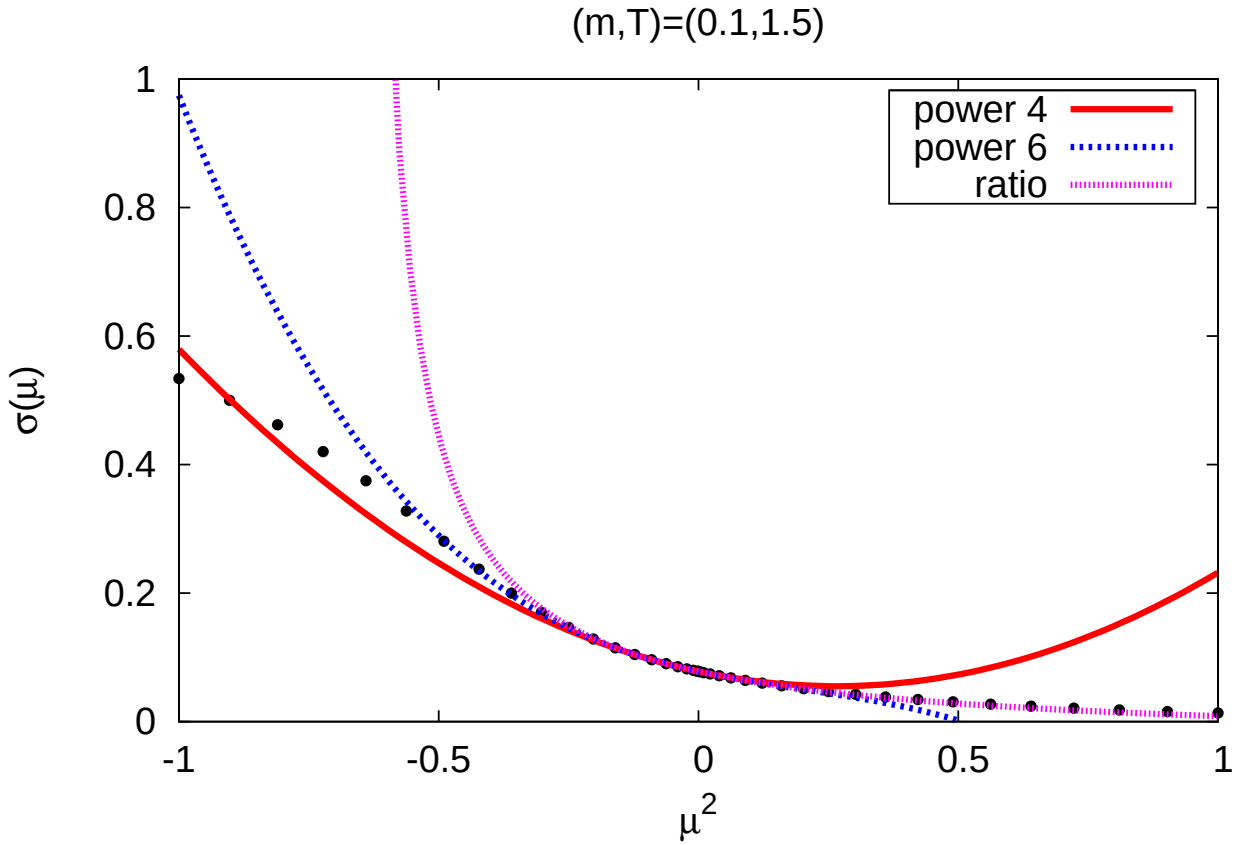

Figure 9: Same as in Fig.8. For "data" in imaginary μ region, polynomials and ratio fits are employed.

∴ The ratio type of fit works very well.

5. Summary and discussion

Summary

- 2-color CRMM in the real μ region

$$\begin{cases} -m = 0: & \text{diquark condensate and symmetric phases are separated} \\ & \quad \text{by a 2nd order phase transition} \\ -m \neq 0: & \text{chiral condensate phase emerges in the small } \mu \text{ region} \end{cases}$$

- 2-color CRMM in the imaginary μ region

$$\begin{cases} -m = 0: & \text{chiral condensate and symmetric phases are separated} \\ & \quad \text{by a 2nd order phase transition} \\ -m \neq 0: & \text{chiral conndensate phase realizes in the imaginary } \mu \text{ region} \end{cases}$$

- analytic continuation

  - effective potential and chiral condensate are smoothly connected between real and imaginary μ regions at $\mu = 0$
  - both of polynomial and ratio types of fitting for chiral condensate are good up to $(\mu G)^2 \simeq 0.089$ in the low temperature region
  - ratio type of fitting works very well in the high temperature region

Outlook

- lack of Roberge-Weiss symmetry $\longrightarrow$ M. A. Halasz (2000)
- investigation of higher Matsubara frequency effects $\longrightarrow$ B. Vanderheyden and A. D. Jackson (2001)
- study of 3-color CRMM with baryon and isospin chemical potentials

- **phase diagram**

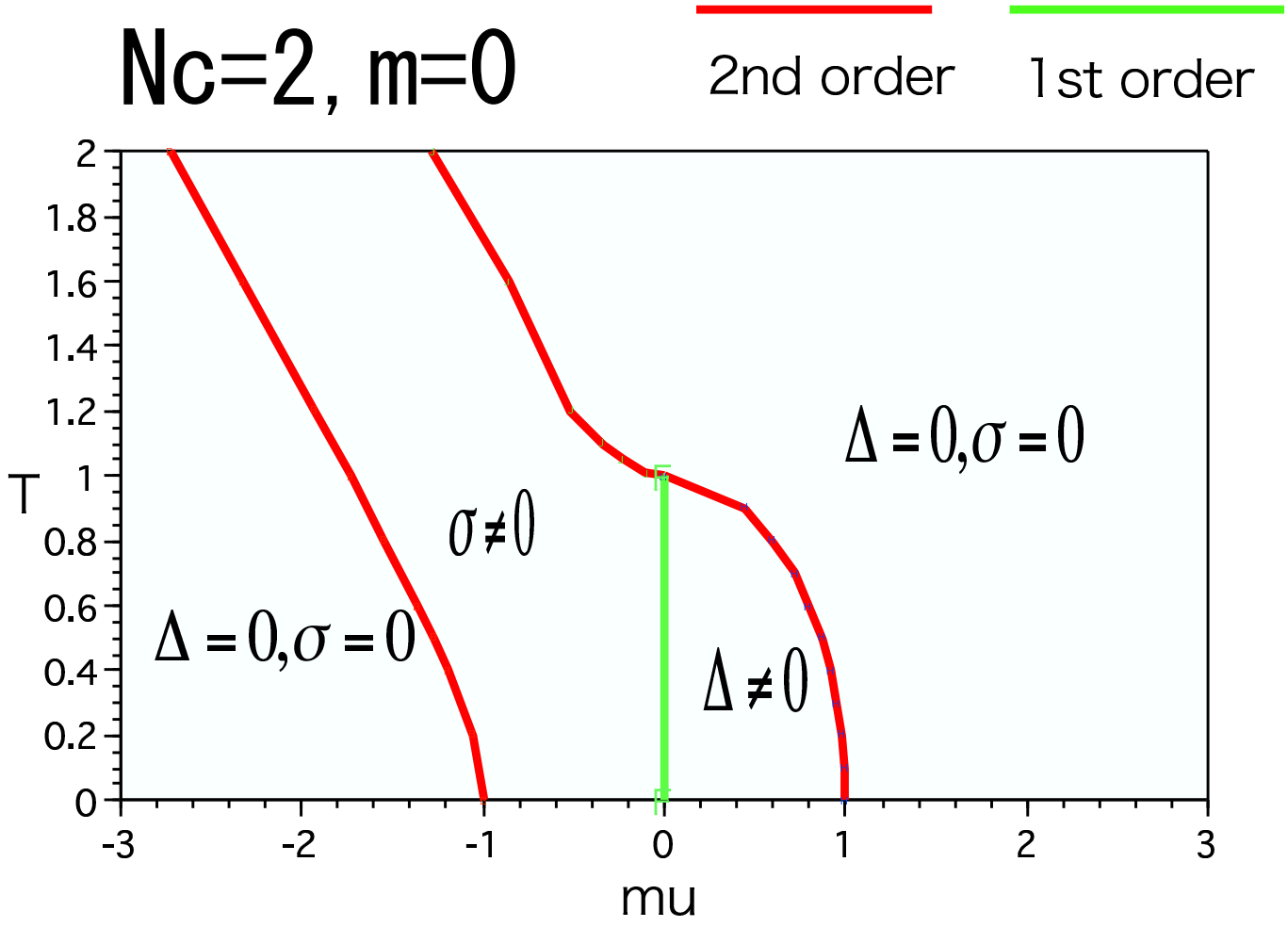

Figure 10: Phase structure for $m = 0.0$ in μ/μ_I-T plane.

- **chiral condensate**

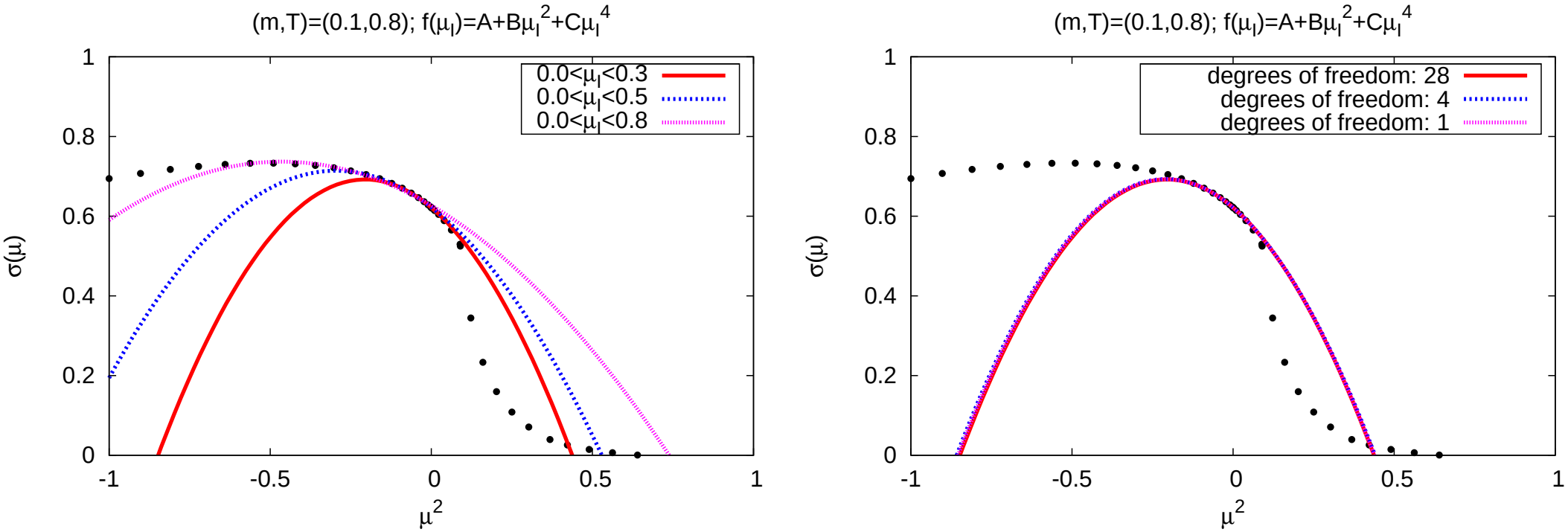

Figure 11: Chiral condensate for $m = 0.1$ and $T = 0.8$(low temperature). The 2nd power fits in μ^2 are employed. In the left side of the figure, the range of "data" points is changed in the imaginary μ region, and in the right side of the figure, the number of "data" points is changed in $0.0 \leq \phi \leq 0.3$.

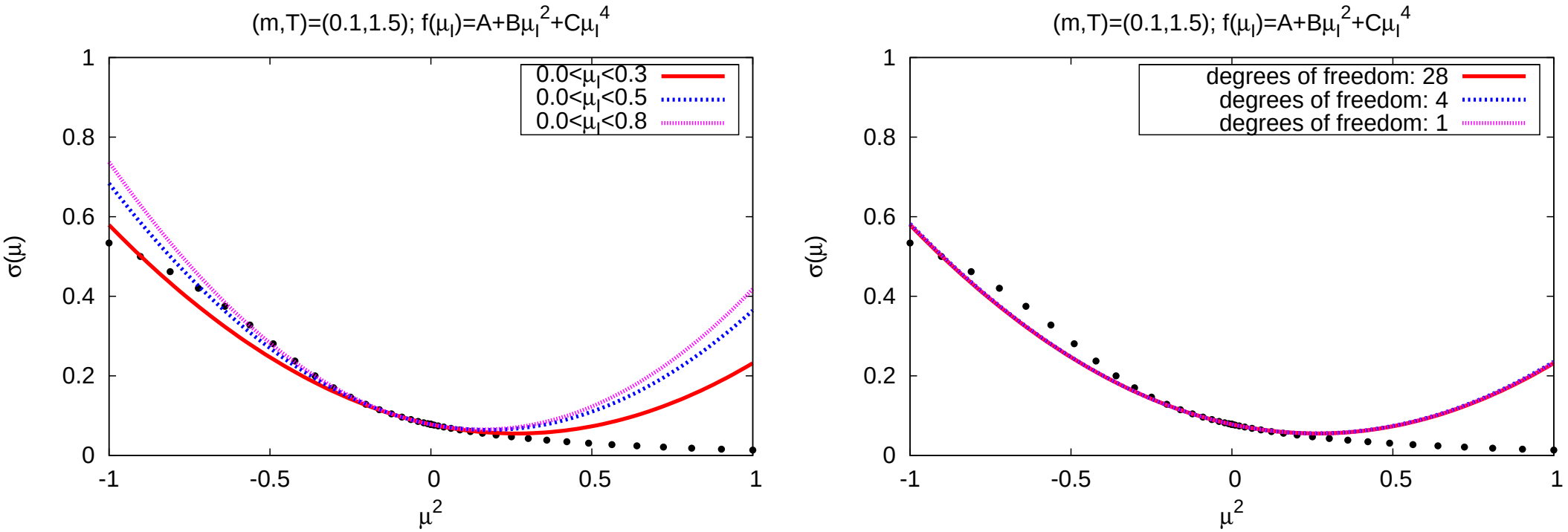

Figure 12: Chiral condensate for $m = 0.1$ and $T = 1.5$(high temperature).